JOURNAL OF COMPUTATIONAL PHYSICS 64, 97–111 (1986)

A Petrov–Galerkin Finite Element Method for Solving the Neutron Transport Equation*

A. GREENBAUM AND J. M. FERGUSON

Lawrence Livermore National Laboratory, Livermore, California 94550

Received May 3, 1984; revised December 13, 1984

A finite element method using different trial and test spaces is introduced for solving the neutron transport equation in spherical geometry. It is shown that the widely used discrete ordinates method can also be thought of as such a finite element technique, in which integrals appearing in the difference equations are replaced by one-point Gauss quadrature formulas (midpoint rule). Comparison of accuracy between the new method and the discrete ordinates method is discussed, and numerical examples are given to illustrate the greater accuracy of the new technique.

INTRODUCTION

The neutron transport equation in spherical geometry can be written in the form

$$\frac{1}{v}\frac{\partial \psi}{\partial t}+\mu\frac{\partial \psi}{\partial r}+\frac{1-\mu^2}{r}\frac{\partial \psi}{\partial \mu}+\Sigma\psi=S, \qquad 0<r<R_{\max}, \quad -1<\mu<1, \tag{1}$$

where $\psi \equiv \psi(r, \mu, t)$ represents the unknown neutron flux at radius r, angle $\cos^{-1}\mu$, and time t. Various discretizations have been used to solve Eq. (1), one of the most popular being the method of discrete ordinates [1]. Galerkin finite element approximations—using, for example, continuous piecewise bilinear functions as trial and test functions—have also been considered [2], but these have the disadvantage of yielding a large, implicit system of linear equations that must be solved at each time step. Finite element techniques using discontinuous approximation functions have recently been studied [3], but these also appear to require significantly more work per grid point than the discrete ordinates method.

In this paper we consider a Petrov–Galerkin finite element approximation (one in which the trial space and test space are different), and illustrate numerically that

* This work was performed under the auspices of the U.S. Department of Energy by Lawrence Livermore National Laboratory under Contract W-7405-ENG-48. Partial support for the first author was provided by the Applied Mathematical Sciences subprogram of the Office of Energy Research, U.S. Department of Energy.

0021-9991/86 $3.00

it gives the optimal order of accuracy without requiring the solution of a large, implicit linear system. (A preliminary account of some of this work appears in Ref. [4].) It is shown that the discrete ordinates method results if the integrals appearing in the finite element equations are replaced by one-point Gauss quadrature (midpoint rule) approximations. The effect of such a replacement on the accuracy of the computed solution is also discussed.

The Method

Given grid points $\{(r_j, \mu_k),\ j=1,...,NR,\ k=1,...,NMU\}$ the finite element approximation $\hat{\psi}(r, \mu, t)$ for Eq. (1) will be taken to be a *continuous piecewise bilinear* function in r and μ for which the following relations hold:

$$\text{(a)}\quad \int_{r_j}^{r_{j+1}} r^2\,dr \int_{\mu_k}^{\mu_{k+1}} d\mu \left[\frac{1}{v}\frac{\partial\hat{\psi}}{\partial t} + \mu\frac{\partial\hat{\psi}}{\partial r} + \frac{1-\mu^2}{r}\frac{\partial\hat{\psi}}{\partial\mu} + \Sigma\hat{\psi}\right] = \int_{r_j}^{r_{j+1}} r^2\,dr \int_{\mu_k}^{\mu_{k+1}} d\mu\, S, \qquad \begin{matrix} j=1,...,NR-1, \\ k=1,...,NMU-1, \end{matrix} \tag{2}$$

$$\text{(b)}\quad \int_{r_j}^{r_{j+1}} r^2\,dr \left[\frac{1}{v}\frac{\partial\hat{\psi}}{\partial t} - \frac{\partial\hat{\psi}}{\partial r} + \Sigma\hat{\psi}\right] = \int_{r_j}^{r_{j+1}} r^2\,dr\, S, \qquad \begin{matrix} j=1,...,NR-1, \\ \mu=-1. \end{matrix}$$

The solution of Eq. (1) is uniquely determined by initial conditions

$$\psi(r, \mu, 0) \quad \text{given} \tag{3}$$

and boundary conditions

$$\begin{aligned} &\text{(a)} && \psi(R_{\max}, \mu, t) && \text{given for} \quad \mu \leqslant 0,\ t>0, \\ &\text{(b)} && \psi(0, \mu, t) = \psi(0, -\mu, t) && \text{for} \quad \mu>0,\ t>0. \end{aligned} \tag{4}$$

Likewise, these conditions (or conditions involving the piecewise bilinear interpolants of the given functions) will be enforced upon the approximate solution $\hat{\psi}(r, \mu, t)$. We have chosen a reflecting boundary condition (Eq. (4b)) because it has been used extensively in various discrete ordinates formulations [cf. 1]. It is not the only possible choice, or necessarily the best, but a discussion of this issue is beyond the scope of this paper.

In Eqs. (2), all of the integrals involving r and μ can be evaluated *analytically*, since $\hat{\psi}$ is simply a bilinear function of these variables. Thus, the only approximation in the finite element method is introduced by the bilinear representation within each zone. The use of functions linear in μ guarantees, in particular, that the approximation approaches the diffusion limit correctly.

In the terminology of finite elements, then, $\hat{\psi}(r, \mu, t)$ is that function in $T_1 \equiv$ {continuous, piecewise bilinear functions}, for which the relations

$$\text{(a)} \qquad \langle L\hat{\psi}, \chi \rangle = \langle S, \chi \rangle,$$

$$L \equiv \frac{1}{v}\frac{\partial}{\partial t} + \mu \frac{\partial}{\partial r} + \frac{1-\mu^2}{r}\frac{\partial}{\partial \mu} + \Sigma \tag{5}$$

$$\langle f, g \rangle \equiv \int_0^{R_{\max}} r^2\, dr \int_{-1}^{1} d\mu\, fg$$

$$\text{(b)} \qquad \langle L\hat{\psi}, \chi \rangle_{-1} = \langle S, \chi \rangle_{-1}$$

$$\langle f, g \rangle_{-1} \equiv \int_0^{R_{\max}} r^2\, dr\, f(r, -1)\, g(r, -1),$$

hold, for all functions χ in $T_2 \equiv \{\text{piecewise constants (in zones)}\} \cup \{\text{piecewise constants (in intervals along } \mu = -1)\}$. Since T_1 and T_2 are different, this is called a *Petrov–Galerkin* finite element approximation.

To compute the approximate solution determined by (2)–(4), we first express the bilinear function $\hat{\psi}$ in the form

$$\text{(a)} \qquad \hat{\psi}(r, \mu, t) = \frac{1}{(\Delta r)(\Delta \mu)} [\hat{\psi}_{j,k}(t)(r_{j+1} - r)(\mu_{k+1} - \mu)$$

$$+ \hat{\psi}_{j+1,k}(t)(r - r_j)(\mu_{k+1} - \mu) + \hat{\psi}_{j+1,k+1}(t)(r - r_j)(\mu - \mu_k)$$

$$+ \hat{\psi}_{j,k+1}(t)(r_{j+1} - r)(\mu - \mu_k)],$$

$$r_j \leqslant r \leqslant r_{j+1},\ \mu_k \leqslant \mu \leqslant \mu_{k+1}, \tag{6}$$

$$\text{(b)} \quad \hat{\psi}(r, -1, t) = \frac{1}{\Delta r} [\hat{\psi}_{j+1,1}(t)(r - r_j) + \hat{\psi}_{j,1}(t)(r_{j+1} - r)],$$

$$r_j \leqslant r \leqslant r_{j+1},\ \mu = -1,$$

where $\hat{\psi}_{p,q}(t) \equiv \hat{\psi}(r_p, \mu_q, t)$, $\quad p = j, j+1,\ q = k, k+1,$

$$\Delta r \equiv r_{j+1} - r_j, \qquad \Delta \mu \equiv \mu_{k+1} - \mu_k.$$

Substituting this expression into (2) and evaluating necessary derivatives, we obtain a system of *ordinary differential equations* for the unknown flux values $\hat{\psi}_{j,k}(t)$ at the grid points (r_j, μ_k). These ordinary differential equations can be solved using any of several standard difference methods. For our program, we used a simple centered difference scheme in time (Crank–Nicholson). This is almost equivalent (as we shall see later) to using the same Petrov–Galerkin finite element technique for the time variable as well.

To compute the approximate solution $\hat{\psi}$ at time t^{n+1}, then, we must compute the derivatives $d\hat{\psi}_{j,k}/dt$ at time $t^{n+1/2}$ and then set

$$\hat{\psi}_{j,k}(t^{n+1}) = \hat{\psi}_{j,k}(t^n) + (\Delta t)\frac{d\hat{\psi}_{j,k}}{dt}_{t=t^{n+1/2}}, \qquad \Delta t \equiv t^{n+1} - t^n. \tag{7}$$

We compute the derivatives $(d\hat{\psi}_{j,k}/dt)(t^{n+1/2})$, starting along the line $\mu = -1$. Given the values of $\hat{\psi}_{NR,1}(t)$, we can determine $(d\hat{\psi}_{NR,1}/dt)(t^{n+1/2})$, and then Eq. (2b) can be used to calculate $(d\hat{\psi}_{NR-1,1}/dt)(t^{n+1/2})$. In this way, Eq. (2b) is used to march down the line $\mu = -1$, from $r_{NR} = R_{\max}$ to $r_1 = 0$. Now, given the value of the approximate solution (or its time derivative) at three corners of a zone, Eq. (2a) can be used to determine the value at the fourth corner. Thus, knowing $(d\hat{\psi}_{NR,k}/dt)(t^{n+1/2})$, $k = 1,\ldots, (NMU+1)/2$ and $(d\hat{\psi}_{j,1}/dt)(t^{n+1/2})$, $j = 1,\ldots, NR$, we can use (2a) to compute $(d\psi_{NR-1,2}/dt)(t^{n+1/2})$. With this, we can then evaluate the derivative at (r_{NR-1}, μ_3) or (r_{NR-2}, μ_2), etc. When solutions have been calculated at all grid points with $\mu \leqslant 0$, we then apply the boundary condition (4b) to obtain the solution at $r = 0$ for $\mu > 0$. We then use Eq. (2a) to march back through the grid, determining solution values for positive μ. Thus the order in which solutions are obtained is equivalent to that used in the discrete ordinates method. The number of numerical operations for a given grid is equivalent to that required by the discrete ordinates method.

The difference equations for carrying out this process can be written in the form

(a)
$$\begin{aligned}\hat{\psi}_{j,k+1}^{(n+1)} = [&4V^* S_{j,k} - a_{j,k}\hat{\psi}_{j,k}^{(n)} - b_{j,k}\hat{\psi}_{j+1,k}^{(n)} \\ &- c_{j,k}\hat{\psi}_{j+1,k+1}^{(n)} - d_{j,k}\hat{\psi}_{j,k+1}^{(n)} - e_{j,k}\hat{\psi}_{j,k}^{(n+1)} \\ &- f_{j,k}\hat{\psi}_{j+1,k}^{(n+1)} - g_{j,k}\hat{\psi}_{j+1,k+1}^{(n+1)}]/h_{j,k},\end{aligned} \tag{8}$$

where

$$S_{j,k} = \frac{1}{\Delta r\,\Delta\mu}\int_{r_j}^{r_{j+1}} r^2\,dr \int_{\mu_k}^{\mu_{k+1}} d\mu\, S(r, \mu, t^{n+1/2}),$$

$$a_{j,k} = \frac{1}{2}\alpha_{j,k} - \frac{1}{\Delta t}(r^2)_2,$$

$$b_{j,k} = \frac{1}{2}\beta_{j,k} - \frac{1}{\Delta t}(r^2)_3,$$

$$c_{j,k} = \frac{1}{2}\gamma_{j,k} - \frac{1}{\Delta t}(r^2)_3,$$

$$d_{j,k} = \frac{1}{2}\delta_{j,k} - \frac{1}{\Delta t}(r^2)_2,$$

$$e_{j,k} = \frac{1}{2}\alpha_{j,k} + \frac{1}{\Delta t}(r^2)_2,$$

$$f_{j,k}=\frac{1}{2}\beta_{j,k}+\frac{1}{\Delta t}(r^2)_3,$$

$$g_{j,k}=\frac{1}{2}\gamma_{j,k}+\frac{1}{\Delta t}(r^2)_3,$$

$$h_{j,k}=\frac{1}{2}\delta_{j,k}+\frac{1}{\Delta t}(r^2)_2,$$

$$\alpha_{j,k}=-\frac{2V}{\Delta r}(r^2)_1(\mu)_1-\frac{2V}{\Delta\mu}(1-(\mu^2)_1)(r)_1+\frac{2V}{\Delta r}(\sigma)_2.$$

$$\beta_{j,k}=\frac{2V}{\Delta r}(r^2)_1(\mu)_1-\frac{2V}{\Delta\mu}(1-(\mu^2)_1)(r)_2+\frac{2V}{\Delta r}(\sigma)_1,$$

$$\gamma_{j,k}=\frac{2V}{\Delta r}(r^2)_1(\mu)_2+\frac{2V}{\Delta\mu}(1-(\mu^2)_1)(r)_2+\frac{2V}{\Delta r}(\sigma)_1,$$

$$\delta_{j,k}=-\frac{2V}{\Delta r}(r^2)_1(\mu)_2+\frac{2V}{\Delta\mu}(1-(\mu^2)_1)(r)_1+\frac{2V}{\Delta r}(\sigma)_2,$$

$$(r)_1=\frac{r_{j+1}+2r_j}{3},\qquad (r)_2=\frac{2r_{j+1}+r_j}{3}$$

$$(r^2)_1=\frac{r_{j+1}^2+r_{j+1}r_j+r_j^2}{3},\qquad (r^2)_2=\frac{r_{j+1}^2+2r_{j+1}r_j+3r_j^2}{6},$$

$$(r^2)_3=\frac{3r_{j+1}^2+2r_{j+1}r_j+r_j^2}{6},$$

$$(\mu)_1=\frac{\mu_{k+1}+2\mu_k}{3},\qquad (\mu)_2=\frac{2\mu_{k+1}+\mu_k}{3},$$

$$(\mu^2)_1=\frac{\mu_{k+1}^2+\mu_{k+1}\mu_k+\mu_k^2}{3},$$

$$(\sigma)_1=\frac{1}{\Delta r}\int_{r_j}^{r_{j+1}} r^2\sum(r,t^{n+1/2})(r-r_j)\,dr,$$

$$(\sigma)_2=\frac{1}{\Delta r}\int_{r_j}^{r_{j+1}} r^2\sum(r,t^{n+1/2})(r_{j+1}-r)\,dr,$$

for $-1<\mu\leqslant 0$, and a similar formula gives $\hat{\Psi}_{j+1,k+1}^{(n+1)}$ in terms of $\hat{\Psi}_{j,k+1}^{(n+1)}$, $\hat{\Psi}_{j,k}^{(n+1)}$, and $\hat{\Psi}_{j+1,k}^{(n+1)}$, when μ is greater than zero. Along the line $\mu=-1$, the equations are

(b)
$$\hat{\Psi}_{j,1}^{(n+1)}=[2v*S_{j,1}-c_{j,1}\hat{\Psi}_{j+1,1}^{(n)}-d_{j,1}\hat{\Psi}_{j,1}^{(n)}-g_{j,1}\hat{\Psi}_{j+1,1}^{(n+1)}]/h_{j,1},\tag{8}$$

where

$$S_{j,1} = \frac{1}{\Delta r}\int_{r_j}^{r_{j+1}} r^2 S(r, -1, t^{n+1/2})\, dr,$$

$$c_{j,1} = \frac{1}{2}\gamma_{j,1} - \frac{1}{\Delta t}(r^2)_3,$$

$$d_{j,1} = \frac{1}{2}\delta_{j,1} - \frac{1}{\Delta t}(r^2)_2,$$

$$g_{j,1} = \frac{1}{2}\gamma_{j,1} + \frac{1}{\Delta t}(r^2)_3,$$

$$h_{j,1} = \frac{1}{2}\delta_{j,1} + \frac{1}{\Delta t}(r^2)_2,$$

$$\gamma_{j,1} = -\frac{2v}{\Delta r}(r^2)_1 + \frac{2v}{\Delta r}(\sigma)_1,$$

$$\delta_{j,1} = \frac{2v}{\Delta r}(r^2)_1 + \frac{2v}{\Delta r}(\sigma)_2.$$

The integrals involving $\sum(r, t^{n+1/2})$ can be approximated (or, in many cases, evaluated exactly), using weighted Gauss quadrature formulae. We used the one-point formula,

$$\int_{r_j}^{r_{j+1}} r^2 \sum(r, t^{n+1/2})(r - r_j)\, dr \approx \Delta r (r^2)_1 \sum(\hat{r}, t^{n+1/2})(\hat{r} - r_j),$$

$$\int_{r_j}^{r_{j+1}} r^2 \sum(r, t^{n+1/2})(r_{j+1} - r)\, dr \approx \Delta r (r^2)_1 \sum(\hat{r}, t^{n+1/2})(r_{j+1} - \hat{r}), \tag{9}$$

$$\hat{r} = \frac{3}{r_{j+1}^2 - r_j^2}\left(\frac{r_{j+1}^4 - r_j^4}{4}\right),$$

which is exact provided $\sum$ is constant throughout each zone.

Likewise, the integrals involving the right-hand side function S are approximated using quadrature rules. The function S, however, depends on the solution Ψ. It is given by

$$S(r, \mu, t) = S_{\text{int}}(r, \mu, t) + \tfrac{1}{2}\int_{-1}^{1} \tau_f \Psi(r, \mu', t)\, d\mu'$$

$$+ \tfrac{1}{2}\int_{-1}^{1} \tau_0 \Psi(r, \mu', t)\, d\mu'$$

$$+ \tfrac{3}{2}\mu \int_{-1}^{1} \tau_1 \Psi(r, \mu', t)\, \mu'\, d\mu', \tag{10}$$

where $S_{\text{int}}(r, \mu, t)$ is a given internal source, τ_f represents a known fission source, and τ_0 and τ_1 are known terms in the Legendre polynomial expansion of a scattering source.

In this paper we have invoked the $P1$ approximation; i.e., we have represented the scattering distribution with two terms in a Legendre expansion. Additional terms can be added as desired, in a manner analogous to that used in discrete ordinates codes. In the case of the finite element method, the integrals are just sums of integrals of simple polynomials over each zone, and are done analytically.

To estimate the source term S at time $t^{n+1/2}$, we linearly extrapolate the solution $\hat{\Psi}$ from times t^{n-1} and t^n to time $t^{n+1/2}$. (On the first time step S is estimated using the initial value of $\hat{\Psi}$.) Using this estimate, we then solve Eqs. (8) to determine an approximation for $\hat{\Psi}$ at time t^{n+1}. This is averaged with the known solution $\hat{\Psi}$ at time t^n, to obtain a new approximation for $\hat{\Psi}$ at time $t^{n+1/2}$. If this approximation is close enough to the previous estimate, then $\hat{\Psi}(r, \mu, t^{n+1})$ is accepted as our approximate solution. Otherwise, the value of $\hat{\Psi}$ at time $t^{n+1/2}$ is used to calculate an improved source term, and Eqs. (8) are solved again using this new right-hand side. This iteration is repeated until a converged result for the approximate solution $\hat{\Psi}(r, \mu, t^{n+1})$ is obtained.

Comparison with the Discrete Ordinates Method

The widely used discrete ordinates method for solving equation (1) results from writing the equation in conservative form

$$\frac{1}{v}\frac{\partial \Psi}{\partial t}+\frac{\mu}{r^2}\frac{\partial(r^2\Psi)}{\partial r}+\frac{1}{r}\frac{\partial((1-\mu^2)\,\Psi)}{\partial \mu}+\sum \Psi = S, \tag{11}$$

and then replacing all derivatives by difference approximations. In the most common method, called diamond differencing [1], the derivatives are replaced by centered differences, giving second-order accuracy. Making this replacement and integrating each side of Eq. (11) over a zone $[r_j, r_{j+1}]\times[\mu_k, \mu_{k+1}]$, gives rise to the following difference equations:

$$\begin{aligned}
&\frac{1}{v}\frac{\tilde{\Psi}(\bar{r}, \bar{\mu}, t^{n+1})-\tilde{\Psi}(\bar{r}, \bar{\mu}, t^n)}{\Delta t}(\overline{r^2})(\Delta r)(\Delta \mu)\\
&\quad+\frac{r_{j+1}^2\,\tilde{\Psi}(r_{j+1}, \bar{\mu}, t^{n+1/2})-r_j^2\,\tilde{\Psi}(r_j, \bar{\mu}, t^{n+1/2})}{\Delta r}\bar{\mu}(\Delta \mu)(\Delta r)\\
&\quad+\frac{(1-\mu_{k+1}^2)\,\tilde{\Psi}(\bar{r}, \mu_{k+1}, t^{n+1/2})-(1-\mu_k^2)\,\tilde{\Psi}(\bar{r}, \mu_k, t^{n+1/2})}{\Delta \mu}\bar{r}(\Delta r)(\Delta \mu),\\
&\quad+\sum(\bar{r}, t^{n+1/2})\,\tilde{\Psi}(\bar{r}, \bar{\mu}, t^{n+1/2})(\overline{r^2})(\Delta r)(\Delta \mu)\\
&=S(\bar{r}, \bar{\mu}, t^{n+1/2})(\overline{r^2})(\Delta r)(\Delta \mu),
\end{aligned} \tag{12}$$

where

$$\bar{r} = \frac{r_{j+1} + r_j}{2}, \qquad (\overline{r^2}) = \frac{r_{j+1}^2 + r_{j+1} r_j + r_j^2}{3},$$

$$\Delta r = r_{j+1} - r_j,$$

$$\bar{\mu} = \frac{\mu_{k+1} + \mu_k}{2}, \qquad \Delta\mu = \mu_{k+1} - \mu_k.$$

Equation (12) is strictly correct only for the case in which the "center" of each angular bin is taken to be the arithmetic mean of the boundaries. In the important case where Gauss–Legendre quadratures are used to represent the angles, the discrete angles are not at the zone centers. It will be shown below that the use of such sets greatly enhances the accuracy of the discrete ordinates method. This effect will be discussed and accounted for in the numerical examples. To show the analytic connection between the discrete ordinates and finite element methods, however, we will use the special form of discrete ordinates given above.

Given the values of $\tilde{\Psi}(r_{j+1}, \bar{\mu}, t^{n+1/2})$(or $\tilde{\Psi}(r_j, \bar{\mu}, t^{n+1/2})$ if $\mu > 0$) and $\tilde{\Psi}(\bar{r}, \mu_k, t^{n+1/2})$, Eq. (12) is solved for the value of $\tilde{\Psi}(\bar{r}, \bar{\mu}, t^{n+1/2})$, after making the substitutions

$$\begin{aligned}
\tilde{\Psi}(\bar{r}, \bar{\mu}, t^{n+1}) &= 2\tilde{\Psi}(\bar{r}, \bar{\mu}, t^{n+1/2}) - \tilde{\Psi}(\bar{r}, \bar{\mu}, t^n), \\
\tilde{\Psi}(r_j, \bar{\mu}, t^{n+1/2}) &= 2\tilde{\Psi}(\bar{r}, \bar{\mu}, t^{n+1/2}) - \tilde{\Psi}(r_{j+1}, \bar{\mu}, t^{n+1/2}), \\
\tilde{\Psi}(\bar{r}, \mu_{k+1}, t^{n+1/2}) &= 2\tilde{\Psi}(\bar{r}, \bar{\mu}, t^{n+1/2}) - \tilde{\Psi}(\bar{r}, \mu_k, t^{n+1/2}).
\end{aligned} \tag{13}$$

These same relations are then used to obtain the values of $\tilde{\Psi}(r_j, \bar{\mu}, t^{n+1/2})$(or $\tilde{\Psi}(r_{j+1}, \bar{\mu}, t^{n+1/2})$ if $\mu > 0$) and $\tilde{\Psi}(\bar{r}, \mu_{k+1}, t^{n+1/2})$, and finally to obtain corresponding values at time t^{n+1}.

The difference equations for the finite element approximation result from assuming the solution Ψ to be bilinear in r and μ in each zone (so that, e.g., relations (13) hold), and then integrating each side of Eq. (1) or, equivalently, Eq. (11) to obtain

$$\begin{aligned}
&\int_{r_j}^{r_{j+1}} r^2\, dr \int_{\mu_k}^{\mu_{k+1}} \frac{1}{v} \frac{\partial \hat{\Psi}}{\partial t}\, d\mu \\
&\quad + \int_{\mu_k}^{\mu_{k+1}} \mu [r_{j+1}^2 \hat{\Psi}(r_{j+1}, \mu, t) - r_j^2 \hat{\Psi}(r_j, \mu, t)]\, d\mu \\
&\quad + \int_{r_j}^{r_{j+1}} r [(1 - \mu_{k+1}^2)\, \hat{\Psi}(r, \mu_{k+1}, t) - (1 - \mu_k^2)\, \hat{\Psi}(r, \mu_k, t)]\, dr \\
&\quad + \int_{r_j}^{r_{j+1}} r^2 \sum (r, t)\, dr \int_{\mu_k}^{\mu_{k+1}} \hat{\Psi}(r, \mu, t)\, d\mu \\
&= \int_{r_j}^{r_{j+1}} r^2\, dr \int_{\mu_k}^{\mu_{k+1}} S(r, \mu, t)\, d\mu.
\end{aligned} \tag{14}$$

If the integrals in Eq. (14) are approximated using the midpoint rule,

$$\int_a^b f(x)\, w(x)\, dx \approx f\left(\frac{b+a}{2}\right) \int_a^b w(x)\, dx,$$

then the resulting difference equations,

$$\begin{aligned}
&\frac{1}{v}\frac{\partial \tilde{\Psi}(\bar{r}, \bar{\mu}, t)}{\partial t}(\overline{r^2})(\Delta r)(\Delta \mu) \\
&\quad + \bar{\mu}(r_{j+1}^2 \tilde{\Psi}(r_{j+1}, \bar{\mu}, t) - r_j^2 \tilde{\Psi}(r_j, \bar{\mu}, t))(\Delta \mu) \\
&\quad + \bar{r}((1-\mu_{k+1}^2)\, \tilde{\Psi}(\bar{r}, \mu_{k+1}, t) - (1-\mu_k^2)\, \tilde{\Psi}(\bar{r}, \mu_k, t))(\Delta r) \\
&\quad + \sum(\bar{r}, t)\, \tilde{\Psi}(\bar{r}, \bar{\mu}, t)(\overline{r^2})(\Delta r)(\Delta \mu) \\
&= S(\bar{r}, \bar{\mu}, t)(\overline{r^2})(\Delta r)(\Delta \mu)
\end{aligned} \tag{15}$$

are seen to be exactly the same as those in (12), once the substitution (7) is made for $\partial \tilde{\Psi}/\partial t$. Thus, the discrete ordinates method is equivalent to a modified finite elements method, in which integrals appearing in the difference equations have been replaced by one-point Gauss quadrature formulae. Again, we emphasize that comparison of angular terms assumes that the discrete angles are at the midpoints of the angular zones, a condition that does not hold for the popular Gauss–Legendre quadrature. The effects of this are discussed further in the following section.

The order of error in the midpoint rule approximation is the same as that in approximation of an arbitrary function by a piecewise bilinear function, i.e., $O((\Delta r)^2 + (\Delta \mu)^2)$. For this reason, we might expect that the finite element approximation and the discrete ordinates approximation would have the same order of accuracy. Numerical experiments support this hypothesis.

Both the diamond difference scheme and the finite element method can generate negative fluxes under appropriate conditions. In cases where negative fluxes cannot be tolerated, most discrete ordinates codes use a "negative flux fixup," which generally involves the introduction of a first order scheme which forces positivity. Similar fixups can be used for the finite element method, using elements which will not go negative in those special cases. A discussion of these techniques, however, will be deferred to a later paper.

While a detailed error analysis of the two methodes is beyond the scope of this paper, we can gain some insight into the relative performance of the two methods by considering the errors made in the various approximations. To this end we will consider a time-independent problem, since both methods use the same time differencing scheme, and we will assume that the right-hand side function S is known (independent of Ψ). In this case, then, the true solution $\Psi(r, \mu)$ satisfies the equations

$$\int_{\mu_k}^{\mu_{k+1}} \mu[r_{j+1}^2 \Psi(r_{j+1}, \mu) - r_j^2 \Psi(r_j, \mu)]\, d\mu$$

$$+ \int_{r_j}^{r_{j+1}} r[(1-\mu_{k+1}^2)\, \Psi(r, \mu_{k+1}) - (1-\mu_k^2)\, \Psi(r, \mu_k)]\, dr$$

$$+ \int_{r_j}^{r_{j+1}} r^2 \sum(r) \int_{\mu_k}^{\mu_{k+1}} \Psi(r, \mu)\, d\mu = \int_{r_j}^{r_{j+1}} r^2\, dr \int_{\mu_k}^{\mu_{k+1}} S(r, \mu)\, d\mu,$$

$$j = 1, \ldots, NR-1,\ k = 1, \ldots, NMU-1. \tag{16}$$

If we replace the function Ψ by a piecewise bilinear function, say its bilinear interpolant, then it can be shown using Taylor's theorem that the integrals in (16) change by an amount that is less than or equal to

$$(\Delta\mu)^3 (\Delta r)\left[\left(\frac{1}{6} R_{\max} + \frac{1}{12} \Sigma_{\max} R_{\max}^2\right) \max_{\mu,r} \left|\frac{\partial^2}{\partial\mu^2} (\Psi(r, \mu))\right| \right.$$

$$\left. + \frac{1}{12} R_{\max}^2 \max_{\mu,r} \left|\frac{\partial^3}{\partial\mu^2\, \partial r} (\Psi(r, \mu))\right|\right]$$

$$+ (\Delta r)^3 (\Delta\mu)\left[\left(\frac{1}{6} R_{\max} + \frac{1}{12} \Sigma_{\max} R_{\max}^2\right) \max_{\mu,r} \left|\frac{\partial^2}{\partial r^2} (\Psi(r, \mu))\right| \right.$$

$$\left. + \frac{1}{12} R_{\max} \max_{\mu,r} \left|\frac{\partial^3}{\partial r^2\, \partial\mu} (\Psi(r, \mu))\right|\right]$$

$$+ (\Delta\mu)^4 \frac{1}{12} R_{\max}^2 \max_{\mu,r} \left|\frac{\partial^3}{\partial\mu^3} (\Psi(r, \mu))\right|$$

$$+ (\Delta r)^4 \frac{1}{12} R_{\max} \max_{\mu,r} \left|\frac{\partial^3}{\partial r^3} (\Psi(r, \mu))\right|. \tag{17}$$

This expression gives an estimate of the amount by which the true solution Ψ fails to satisfy the finite element equations, as the finite element equations are derived by integrating a general piecewise bilinear function.

In the discrete ordinates method, in addition to implicitly assuming a bilinear representation of the solution (as implied by relations (13)), we also use the following integral approximations:

$$\int_a^b f(x)\, dx \approx (b-a) f\left(\frac{b+a}{2}\right),$$

$$\int_a^b f(x)\, x^2\, dx \approx f\left(\frac{b+a}{2}\right) \int_a^b x^2\, dx.$$

The error in approximating the integrals in (16) with such formulas is bounded by

$$(\Delta\mu)^3(\Delta r)\left[\frac{1}{12}R_{\max}\max_{r,\mu}\left|\frac{\partial^2}{\partial\mu^2}(\mu\Psi(r,\mu))\right|\right.$$
$$\left.+\frac{1}{24}\Sigma_{\max}\max_{r,\mu}\left|\frac{\partial^2}{\partial\mu^2}(\Psi(r,\mu))\right|\right]$$
$$+(\Delta r)^3(\Delta\mu)\left[\frac{1}{12}\max_{r,\mu}\left|\frac{\partial^2}{\partial r^2}(r\Psi(r,\mu))\right|\right.$$
$$\left.+\frac{1}{6}R_{\max}\max_{r,\mu}\left|\frac{\partial}{\partial r}(\Sigma(r)\,\Psi(r,\mu))\right|\right]$$
$$+\text{higher order terms} \tag{18}$$

Note that the error terms in (18) are similar to those in (17), except that the new terms involve first derivatives of Ψ or second derivatives of $\mu\Psi$ and $r\Psi$. In some cases the errors committed in approximating the integrals tend to cancel those made in assuming a bilinear representation of the solution. In such cases the discrete ordinates method may achieve a fortuitously high level of accuracy, and, indeed, could outperform the finite element method, in which no such cancellation occurs. This phenomenon is illustrated in the numerical examples of the following section. In general, however, this cancellation cannot be expected, and the sum of the error terms in (17) and (18), or at least the larger of these terms, more accurately indicates the error in the discrete ordinates approximation. Thus, in general, we would expect somewhat greater accuracy from the finite elements approximation, and this also is illustrated in the examples that follow.

Numerical Tests

We have done a series of numerical experiments to verify these conclusions. The results of three test problems illustrate the magnitude of the errors introduced by the discrete ordinates approximations. For each test problem we present three sets of results: (1) variable radial zoning with fine angular zoning; (2) variable angular zoning, uniformly spaced in μ, with very fine radial zoning; and (3) angular zoning based on Gauss–Legendre quadratures, with fine radial zoning. In this last case, the discrete ordinates angles correspond to Gauss–Legendre quadrature and the finite element code uses a nonuniform angular grid for which the zone-averaged angles correspond closely to the Gauss–Legendre quadrature angles.

In all three cases the results are presented as the log of the ratio of the calculated to the correct answers. This quantity is approximately equal to the fractional error in the calculation.

The first test problem, shown in Fig. 1, is a small steady-state source at the center of an absorbing sphere which is two mean free paths thick. No scattering is present.

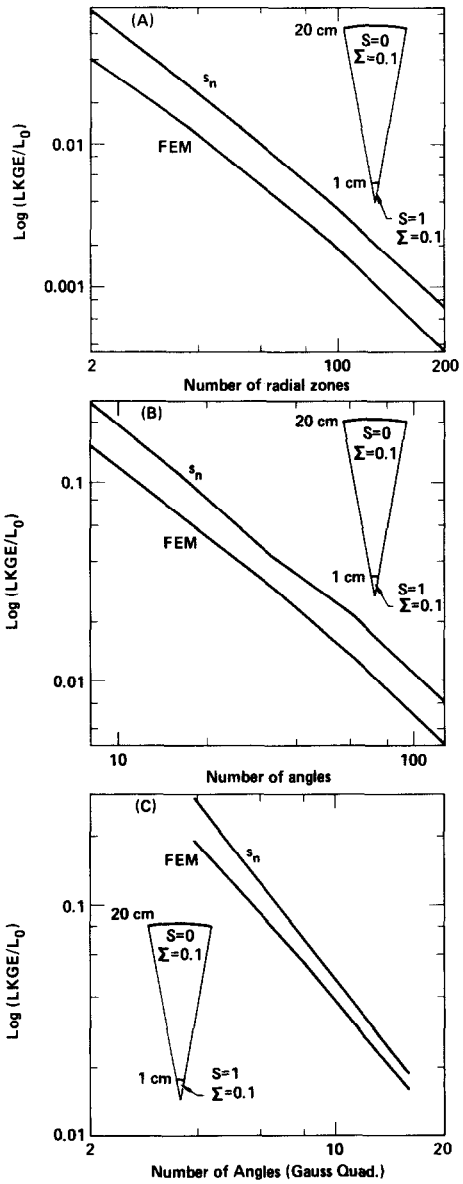

FIG. 1. These curves give the log of the ratio of the calculated to the true leakage for the first test problem (shown in the insets). This quantity is approximately equal to the per cent error for a given mesh size. The source and absorber radii are given in cm, and the macroscopic total cross section Σ, as defined in the text, is given in cm^{-1}. The source S is isotropic, and the materials are pure absorbers. The results for the discrete ordinates method and our finite element method are labelled S_n and FEM, respectively.

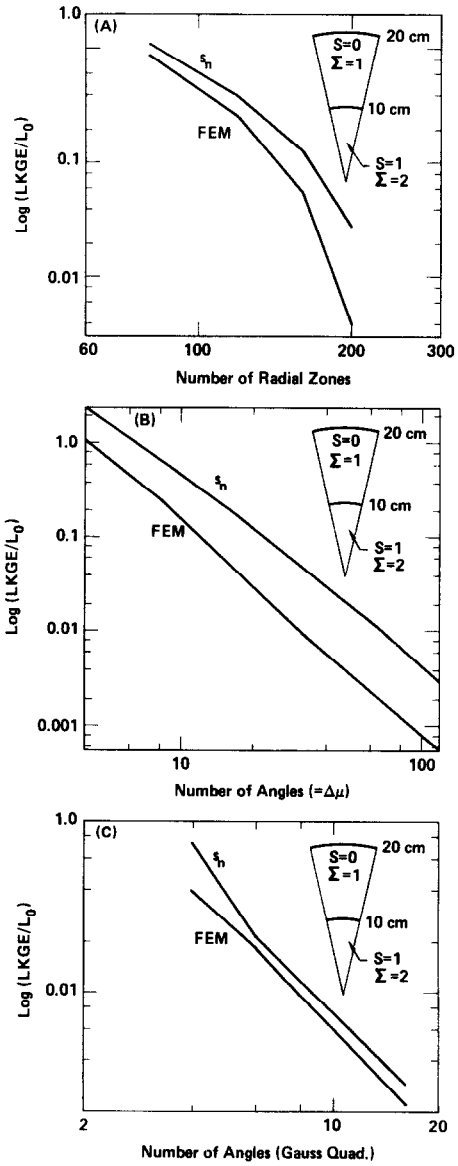

FIG. 2. Results for the second test problem (shown in the insets). The notation is as described for Fig. 1.

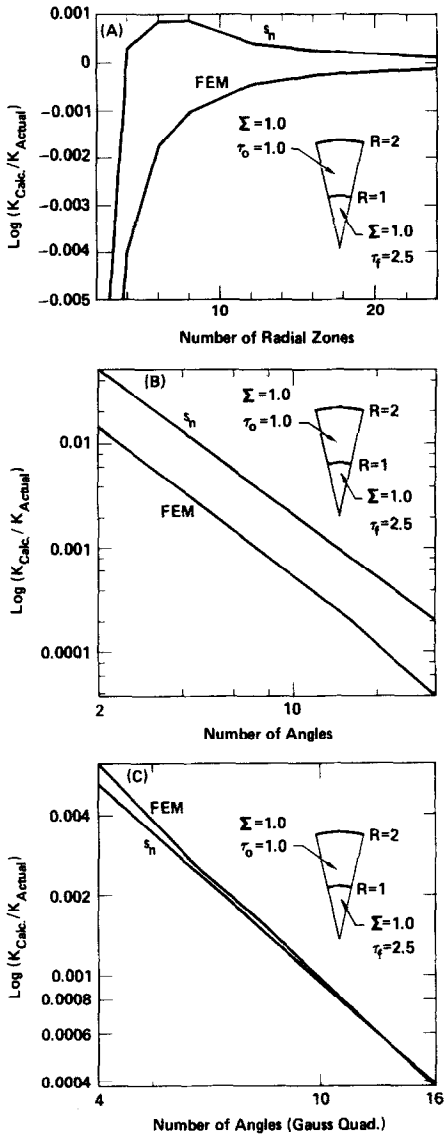

FIG. 3. Results for the third test problem. The notation is as before, except that we now use the criticality, K, as a measure of accuracy. Also, the inner material is "fissile", emitting 2.5 neutrons per collision ($\tau f = 2.5$), and the outer material is a pure isotropic scatterer ($\tau 0 = 1$).

The leakage out of the sphere is taken as a figure of merit. The gain in accuracy of the finite element method over discrete ordinates, for a given number of radial or angular zones, is about a factor of 2. Both methods are improved by use of a Gauss-Legendre quadrature set, with the finite element method advantage reduced to 15–30%

The second test problem is more challenging. It consists of a spherical source with radius 10 cm. embedded in a 20 cm absorber. The absorption cross sections are indicated in the figure caption. In this problem the flux varies by six orders of magnitude across the sphere. The finite element method shows gains in accuracy of about a factor of 3 for reasonable mesh sizes. Again, both methods improve with use of Gauss–Legendre quadratures in angle, with the finite element method advantage reduced to about 15–30%.

The final test problem has quite different properties. The inner sphere consists of a "fissile" material which emits 2.5 neutrons per collision. The outer sphere is a pure isotropic scatterer (scattering cross section = total corss section). In this problem the flux distribution is relatively flat, and the conditions favor the diffusion approximation. The figure of merit for this problem is taken to be the criticality. The errors due to radial zone size are of opposite sign for the two methods, and the discrete ordinates error actually changes sign for crude zoning. The terms neglected in the discrete ordinates approximation apparently are opposite in sign to those terms neglected in assuming a bilinear solution, and tend to cancel. Thus it is possible to find cases in which the discrete ordinates approximation is more accurate than the finite element approximation. This is an exceptional situation, however, and cannot be expected to hold in the general case. In the angular zoning results, the finite element method shows little or no advantage over discrete ordinates for Gauss–Legendre quadratures. Since this test case has a diffusion-like solution over most of the volume, we would expect both methods to do well, since both go to the diffusion limit properly.

To summarize, the test problems indicate that the advantage obtained for the new method is considerable for the radial approximations. For the angular mesh, using Gauss–Legendre quadrature for discrete ordinates, the advantage is smaller but still significant.

REFERENCES

1. B. A. CARLSON AND K. D. LATHROP, "Computing Methods in Reactor Physics," Chap. 3, Gordon & Breach, New York, 1968; references quoted therein.
2. W. F. MILLER, E. E. LEWIS, AND E. C. ROSSOW, *Nuclear Sci. Eng.* **51** (1973), 148; references quoted therein.
3. T. R. HILL, "ONETRAN, A Discrete Ordinates Finite Element Code," LA-5990-M, Los Alamos National Laboratory, 1975.
4. J. M. FERGUSON, *Trans. Amer. Nucl. Soc.* **33** (1979), 328.